Title

Sensitivity of summer stream temperatures to climate variability and riparian reforestation strategies

Authors

Bond, Rosealea M
Stubblefield, Andrew P
Van Kirk, Robert W

Publication Date

2015-09-01

DOI

10.1016/j.ejrh.2015.07.002

Journal of Hydrology: Regional Studies 4 (2015) 267–279

Contents lists available at ScienceDirect

Journal of Hydrology: Regional Studies

journal homepage: www.elsevier.com/locate/ejrh

Sensitivity of summer stream temperatures to climate variability and riparian reforestation strategies

Rosealea M. Bond [a,*,1], Andrew P. Stubblefield [a], Robert W. Van Kirk [b,c]

[a] Department of Forestry and Wildland Resources, Humboldt State University, 1 Harpst Street Arcata, CA 95521, USA
[b] Department of Mathematics, Humboldt State University, 1 Harpst Street Arcata, CA 95521, USA
[c] Henry's Fork Foundation, PO Box 550 512 Main Street Ashton, ID 83420, USA

ARTICLE INFO

Article history:
Received 11 February 2015
Received in revised form 18 June 2015
Accepted 4 July 2015
Available online 23 July 2015

Keywords:
Climate-change
Thermal restoration
Riparian
Cold-water fisheries
Distributed temperature sensing

ABSTRACT

Study region: The Salmon River is the second largest tributary of the Klamath River in northern California, USA. It is a region of steep mountains and diverse conifer forests. Historical land uses including logging, flow diversions, and hydraulic gold mining, have resulted in altered sediment transport regimes, diminished riparian cover and reduced large woody debris. These in turn have altered the thermal regime of the river. Summer stream temperatures commonly exceed salmonid (specifically *Oncorhynchus* spp.) temperature thresholds.
Study focus: Thermal dynamics of a one-kilometer reach of the Salmon River was quantified using distributed temperature sensing fiber-optics (DTS) and *Heat Source* modeling. Stream thermal responses to scenarios of air temperature increase and flow reduction were compared with riparian reforestation simulations to estimate benefits of reforestation.
New hydrological insights: Elevated air temperatures (2 °C, 4 °C, 6 °C) increased mean stream temperature by 0.23 °C/km, 0.45°C/km and .68 °C/km respectively. Reforestation lowered temperatures 0.11–0.12 °C/km for partial and 0.26–0.27 °C/km for full reforestation. Reduced streamflow raised peak stream temperatures in all simulations. Warming could be mitigated by reforestation, however under severe flow reduction and warming (71.0 % reduction, 6 °C air temperature), only half of predicted warming would be reduced by the full reforestation scenario. Land managers should consider reforestation as a tool for mitigating both current and future warming conditions.

1. Introduction

Stream temperature plays a critical role in determining the overall structure and function of stream ecosystems. Temperature directly affects the distribution of fish (Meisner, 1990; Berman and Quinn, 1991; Eaton and Scheller, 1996; Welsh et al., 2001), metabolic and overall growth rates of aquatic organisms (Markarian, 1980; Gregory et al., 2000), and the abiotic conditions – such as gas solubility and solute concentration – that surround them (Matthews and Berg, 1997). Aquatic fauna are particularly vulnerable to changes in the magnitude and duration of elevated stream temperatures due to their limited mobility in the stream environment.

* Corresponding author at: Humboldt State University, 1Harpst Street Arcata, CA 95521, USA. Fax: +1 8314203980.
E-mail address: lea.bond@noaa.gov (R.M. Bond).
[1] Present address: 110 Shaffer Rd. Santa Cruz, CA 95060, USA.

http://dx.doi.org/10.1016/j.ejrh.2015.07.002

Previous research has shown that land management practices both directly and indirectly affect stream temperature. For example, regulated flows have changed the magnitude and extent of peak temperature downstream (Lowney, 2000). Logging and livestock grazing have modified the quantity and quality of riparian vegetation, which buffer the stream from incoming solar radiation (Brown and Krygier, 1970; Armour et al., 1991; Fleischner, 1994; Moore et al., 2005). Land uses that modify stream channel structure and bank stability can also alter the mechanisms of heat transfer within the stream, typically increasing daily maximum temperatures (Poole and Berman, 2001). Stream temperatures are projected to increase with climate-change due to elevated air temperature and changes in precipitation patterns (Eaton and Scheller, 1996; Mohseni et al., 2003; IPCC, 2007; Battin et al., 2007; van Vliet et al., 2013).

Thermal modeling of current and future climate stream thermal regimes is a central area of research to help guide management actions to create and maintain resilient ecological communities. General circulation models (GCMs) have been criticized as too coarse for watershed applications (Solomon et al., 2007). Therefore modeling techniques that link GCM predictions to watershed and reach scales can provide insight into individual stream's vulnerability to climate-change (Hill et al., 2014) and to provide management tools for fish habitat protection (Caissie, 2006). By modeling climate and restoration scenarios, land managers can be more informed about not only the magnitude of expected warming but also the magnitude of warming that might be offset by management actions (Hannah et al., 2008; Seavy et al., 2009; Roth et al., 2010).

Heat Source modeling (Oregon Department of Environmental Quality, ODEQ, 2012, V7.0) was used to investigate the potential thermal benefits of reforesting riparian areas along a reach of the North Fork Salmon River, California, USA that has little vegetation due to legacy land management practices. The model was calibrated with field data collected in July 2012. Climate warming was simulated in multiple scenarios with uniform increases in mean annual air temperatures and reductions in flow. Each warming scenario was then repeated with partial and full riparian reforestation. Warming between the scenarios was then compared to quantify the relative thermal buffering from reforestation.

2. Methods

2.1. Site description

The Salmon River (often referred to as the "Cal-Salmon") is the second largest tributary of the Klamath River in northern California, USA. The Salmon flows east to west and consists of two major forks, North and South, joining at Forks of the Salmon, CA, USA. The entire watershed drains an area of 1945 km^2 with average annual discharge of 1.5 trillion cubic meters (1.2 million acre-ft.) (Elder et al., 2002). The Salmon River enters the Klamath River upstream of the Trinity River sub-basin. The bulk of the Salmon River's precipitation falls between November and May and varies between 203 cm (80 in.) in the headwaters to less than 100 cm (40 in) at the South Fork (Elder et al., 2002). Elevation ranges from 2609 m in the Trinity Alps to 139 m at its mouth. The Salmon River basin is within a tectonically active north-striking fault zone. It is primarily composed of uplifted mafic igneous and oceanic sedimentary deposits (Ando et al., 1983).

The Salmon River basin has a rich cultural heritage. It is part of the ancestral territories of Karuk, Shasta, and Konomihu first nations. Currently, the Klamath National Forest encompasses 90 % of the Salmon River. The Klamath Basin as a whole has experienced widespread anthropogenic stress, primarily from logging, stream-flow diversion, gravel mining, and hydraulic gold mining (National Research Council, 2004). Klamath tributaries were degraded by human activity resulting in lack of stream cover, sedimentation, and absence of large woody debris (LWD) (National Research Council, 2004; National Marine Fisheries Service, 2012). The Salmon River is listed as thermally impaired under California's List of §303(d) Impaired Water Bodies, with mainstem temperature commonly exceeding salmonid temperature thresholds (CA Environmental Protection Agency, 2002). Juvenile salmonids that over-summer in fresh water, including the United States' federally listed coho salmon (*Oncorhynchus kisutch*) are the most at risk to adverse temperatures (Federal Register, 1997). We conducted our study in July to target elevated summer stream temperatures and investigate reforestation as a potential thermal restoration strategy.

The study site consists of a one-kilometer reach of the North Fork Salmon River (41.316528°N, 123.169097°W). It is located one kilometer upstream of Little North Fork Creek confluence, the last major thermal refuge for up-migrating adult salmonids. The reach was broken into ten habitat units corresponding to runs, riffles, and pools as determined by generalized slope/velocity breaks (USDA Forest Service Region 6 Stream Habitat Inventory Level II Protocol, 2006). The study took place over a two week period in July 2012 and the simulation period was five days.

2.2. Field measurements

Heat Source includes multiple modules that simulate open channel hydraulics and flow routing, stream heat transfers, effective shade (topographic and vegetation) and the resulting stream temperature (Boyd and Kasper, 2003). Modeling required a variety of field measurements including meteorology, mainstem discharge, channel cross-sections, and stream temperature at the upstream boundary. Three eKO Pro Series remote weather stations (Envco Environmental Equipment Suppliers, South Pacific) were deployed over the study period. Each station was equipped with an eS2000 eKO Weather Sensor which measured solar radiation, wind speed and direction, air temperature, humidity, barometric pressure, and precipitation, the latter with a tip-bucket rain gauge. The velocity-area procedure was used to measure stream discharge at the upstream end of the study reach (Environmental Protection Agency, 2006). Discharge and depth were measured at 15

Table 1
Initial vegetation heights and densities used in *Heat Source* (tTools) to categorize land cover types from aerial photographs.

Land cover	Height (m)	Density (0–1)
Open water	0.0	0 %
Bare rock/cobble	0.0	0 %
Paved road	0.0	0 %
Large mixed stand	24.0	70 %
Small mixed stand	12.0	70 %
Large conifer stand	27.0	70 %
Small conifer stand	12.0	45 %
Willow/shrub/rock	2.0	30 %

one-meter increments measured with a Swoffer Velocity Meter© Model 2100 (Swoffer Instruments Inc., USA). Measurements were made twice a day, at 09:00 and 16:00 h, for the entire study period.

Channel geometry and cross-sections were collected using the United States Department of Agriculture Forest Service Region 6 Stream Habitat Inventory Level II Protocol (2006). Measurements in each habitat unit included total unit length, maximum longitudinal depth, wetted width, bankfull width, maximum bankfull depth, bankfull depths at 25 %, 50 %, and 75 % of the bankfull width, surface depths at 25 %, 50 %, and 75 % of the wetted width, pool crest depth, and classification of riparian vegetation. Cross-section measurements were taken in three randomly selected locations in all runs and riffle units. Three cross-sections were also measured in pools: a random location at the beginning third of the unit, at the deepest point in the pool, and at the tail water control (i.e., pool tail crest depth).

Stream temperature was measured with distributed temperature sensing technology (DTS). DTS is a method that measures temperature continuously over a glass fiber-optic cable placed in the thalweg of the stream. A detection device in DTS measures Raman back scattering – the proportion of Stokes to anti-Stokes photon scattering through the cable – which change in amplitude in varying thermal conditions (Selker et al., 2006a,b; Tyler et al., 2009). Field applications using DTS cables have improved stream temperature modeling so DTS was chosen for its high spatial and temporal resolution (Westhoff et al., 2007, 2011b; Roth et al., 2010; Matheswaran et al., 2011; Bond 2013). The site layout consisted of a four-channel Oryx remote logging unit (Sensornet LLC. United Kingdom), three 70 amp-hour deep cycle marine batteries connected to two solar panels; two calibration baths, and a 1 km long mini-flat drop fiber-optic cable (AFL Telecommunications, 2007, USA). DTS data was collected at 1m resolution at 15 min intervals. The cable was placed along the stream thalweg (±1 m) and was spliced at the downstream end, creating an internal loop in the cable which collected double ended measurements. DTS goes through a field calibration and post collection processing. Field calibration used the dynamic calibration method which used two calibration baths each with thermocouples and 15-meter coils of cable (Selker et al., 2006a; Tyler et al., 2009). The post-collection processing was completed on both channels using the single-ended method developed by Hausner et al. (2011). The channel with the clearest signal was used for the study analysis.

Riparian vegetation used in *Heat Source* tTool spatial analysis was digitized by hand using ESRI's World Imagery Basemap (2011) in a map view between 1:500 and 1:600 (Boyd and Kasper 2003). In areas where channel boundaries were difficult to distinguish (e.g., topographic shade), aerial photographs taken by Watershed Sciences (2009) were used. Vegetation polygons were assigned vegetation codes with associated height (m) and density (%) (Boyd and Kasper, 2003) (Table 1). Emergent vegetation was set to zero for all polygons due to a lack of vegetation overhanging the banks. Ground-truthing of the digitized vegetation layer was performed by randomly choosing 24 points in the study reach, describing the substrate / vegetation and visually estimating canopy density.

2.3. Model parameterization and simulation procedures

Parameters and constants used in the *Heat Source* model, their values, and their literature reference if applicable are presented (Table 2). Parameters referenced as "measured" or "estimated" were directly measured in the field or estimated from field measurements whose calculations are described in further detail below. "Calibrated" parameters were adjusted to minimize model bias and root mean square error at the downstream-most spatial node (see Section 2.4).

Freeze and Cherry (1979) reported gravel porosity between 0.24 and 0.4. The larger value of the range was chosen because the channel sediment is a mix of gravel and cobble. Both sediment thermal diffusivity and thermal conductivity values were recommended by the *Heat Source* interface to model gravel dominated substrate (Pelletier et al. (2006) cited in ODEQ, 2012). Manning's roughness coefficient was assessed by matching reach descriptions to those provided by Arcement and Schneider (1989). Deep alluvium temperature was estimated as the mean water temperature of three springs measured nearby the study area; two at Kelley's Gulch (40.329717°N, 123.156617°W) and one at White's Gulch (41.303333°N, 123.075233°W) measured on July 24th and 25th 2012, respectively. While most of the parameters used in *Heat Source* were directly measured or estimated, two parameters were used to improve model fit. The thickness of hyporheic/substrate layer and percent hyporheic exchange were included in *Heat Source* simulations to improve predicted evening cooling rates. Parameter values were determined by minimizing model bias and RMSE at the most downstream node.

Table 2
Parameters and constants used in *Heat Source,* value range shows minimum and maximum values measured over the study period.

Constant	Description	Value	Reference
H [%]	Relative Humidity	20 - 100	Measured
T_{air} [°C]	Air temperature	10.2–35.8	Measured
v_{wind} [m s^{-1}]	Wind velocity	0.0 – 3.6	Measured
C [%]	Cloudiness	0 - 100	Estimated
Z [dimensionless]	Mean channel side slope ratio	0.067 - 0.405	Estimated
W_b [m]	Channel bottom width	11.6 - 32.6	Estimated
T_{hyp} [°C]	Deep alluvium temperature	12.31	Estimated
d_{hyp} [m]	Thickness of hyporheic /substrate layer	0.20	Calibrated
Hyp. exchange [%]	Hyporheic exchange	2.00	Calibrated
η [unitless]	Porosity	0.40	Freeze and Cherry (1979)
κ_{sed} [$cm^2 sec^{-1}$]	Sediment thermal diffusivity	0.0064	Pelletier et al. (2006)
K_{sed} [Wm^{-1} °C^{-1}]	Thermal conductivity of sediment	1.57	Pelletier et al. (2006)
n [dimensionless]	Manning's roughness coefficient	0.04	Arcement and Schneider (1989)

Heat Source's flow model simulation partitions the stream into discrete reservoirs that fill from the bottom up. This means that channel bottom width is necessary to simulate flow conditions. Channel bottom width was calculated from measured bankfull widths assuming a trapezoidal channel shape using the equation:

$$W_b = W_{bf} - \left(2Zd_{bf}\right) \tag{1}$$

where W_b is the channel bottom width, W_{bf} is bankfull width, Z is the estimated channel slope ratio, and d_{bf} is the average bankfull depth. Bankfull width was measured once for each habitat unit. All model nodes within each habitat unit were assigned the calculated bottom width.

Channel side slope ratio (Z) was estimated using cross-sections measured in each habitat unit. All model nodes within each habitat unit were assigned this averaged slope ratio.

Percent cloudiness (C) was also estimated as a continuous meteorological input parameter in *Heat Source*. Cloudiness was estimated as a ratio of mean solar radiation (W/m^2) received by the eKO remote weather stations and potential (i.e., no interference including clouds) radiation (W/m^2) estimated by *Heat Source* using the equation:

$$C = \sqrt{1.54\,(1 - \text{received radiation/potential radiation})} \tag{2}$$

Received radiation was measured in the field during the time of study. Potential radiation was estimated by *Heat Source* by reducing all vegetation heights and densities and topology-related features to zero. Elevation was set to a constant value for all model nodes. Then "Shade-a-lator," a package within *Heat Source,* was used to calculate the potential solar radiation. In the past, cloudiness was directly measured and solar radiation was estimated from meteorological conditions (the reader is referred to Boyd and Kasper, 2003; Westhoff et al., 2007 and the corrigendum by Westhoff et al., 2011a, for the governing equations of solar radiation above topographic features). It is important to note that an error in the equation for stream heating contributed by longwave radiation cited by Westhoff et al. (2007, 2011a) was found in the text of the User Manual (Boyd and Kasper, 2003) *not* in the code for *Heat Source* version 7.0 used for this research.

The *Heat Source* model simulated water temperature over the 1-km study reach, at a spatial resolution of 90 m and a temporal resolution of 1 h. The upstream-most node served as the spatial domain boundary, where the stream temperature was fixed at its observed hourly values over the five-day simulation period, and where hourly meteorological and flow conditions were used as model inputs. The model was initialized by simulating hourly temperatures over a five-day period, repeatedly using the temperatures, flow, and meteorological conditions observed on day one as the upstream boundary conditions each day. This allowed the model to reach an equilibrium state for flow and temperature before the model was run with the five-day, time-evolving boundary conditions. These boundary conditions produced simulated temperatures that varied both spatially over the reach and temporally over five full days.

2.4. Data analysis

2.4.1. Heat Source model performance

Before *Heat Source* could be used for model predictions it was necessary to quantify how well the model performed in space and time. We defined model error at each time and each spatial node as

$$\text{error} = \text{predicted temperature} - \text{observed temperature} \tag{3}$$

and calculated four measures of model performance at each of the spatial nodes at which temperatures were simulated (10 in total) The four measures were bias, root mean square error (RMSE), Nash-Sutcliffe Modeling Efficiency (NSE), and log-Nash-Sutcliffe Modeling Efficiency (NSE_{log}) defined, respectively, as:

$$\text{Bias} = \text{mean}\,(\text{predicted} - \text{observed}) \tag{4}$$

Table 3
Table of mean annual air temperature with associated climate models, emissions scenarios, and time horizons (based on Null et al., 2010, 2013).

Increase in mean annual air temperature [°C]	Climate model	Emission scenario	Time horizon
+2	HadCM3	A1FI (higher emissions)	2020–2049
	PCM	B1 (lower emissions)	2070–2099
+4	PCM	A1FI (higher emissions)	2070–2099
+6	HadCM3	A1FI (higher emissions)	2070–2099

$$\text{RMSE} = \sqrt{\text{mean}\left((\text{predicted} - \text{observed})^2\right)} \tag{5}$$

$$\text{NSE} = 1 - \left(\frac{\Sigma\left((\text{predicted} - \text{observed})^2\right)}{\Sigma\left((\text{observed} - \text{mean}(\text{observed}))^2\right)}\right) \tag{6}$$

$$\text{NSE}_{\log} = 1 - \left(\frac{\Sigma\left((\log(\text{predicted}) - \log(\text{observed}))^2\right)}{\Sigma\left(\log(\text{observed}) - \text{mean}(\log(\text{observed}))^2\right)}\right) \tag{7}$$

where means and sums were taken over all hourly observations. NSE was calculated on both raw data and log-transformed data to assess whether large errors skewed measures of model performance. These temporally averaged values were plotted versus location downstream of the top node to assess model performance in space. Model performance generally decreased with distance downstream (see Section 3.1), so temporal analysis of model performance was conducted at the downstream-most node, in order to obtain a "worst case" assessment of error.

Temporal characteristics of model error were made by fitting time series models to the five-day series of hourly temperature errors at the downstream-most node. Based on standard time series diagnostics (Shumway and Stoffer, 2011), we fit eight candidate models that included the mean, first-order autocorrelation, and periodic components. In particular, the inclusion of autocorrelation components ensured that model residuals were independent. Periodicity was modeled with sine and cosine functions with various frequencies ranging between 1 and 11 cycles per day. A null model that included only the mean was also fit. These nine models were ranked using Akaike's Information Criterion, adjusted for small sample size (AICc; Burnham and Anderson, 2004). Residuals from the best model (lowest AICc) met all model assumptions (normal i.i.d.), and this model was used to characterize temporal patterns in error between *Heat Source* and DTS observations.

2.4.2. Predicting thermal impacts from climate-change

A suite of climate-change scenarios regimes with varying air and deep alluvium temperatures and flow regimes were simulated in *Heat Source* and compared to the base model (2012 condition). Air temperatures were increased uniformly (i.e., spatially and temporally) (Diabat et al., 2012) by 2 °C, 4 °C, and 6 °C to reflect forecast mean annual air temperature increases. Deep alluvium temperatures were also increased by the same increment, as groundwater temperatures track average air temperatures. The *Heat Source* equations for atmospheric longwave radiation and land cover longwave radiation include air temperature as an input variable and so increase longwave radiation from these sources accordingly Boyd and Kasper (2003). Changes to humidity and cloudiness in future climates will also influence atmospheric longwave radiation, however changes to these parameters from the base model were not modeled in this study. All other parameters (i.e., meteorological and morphological parameters) remained unchanged (Null et al., 2010). These temperature changes are within the range forecast by climate models for California and represent progressive warming through the end of the 21st century (Table 3, Hayhoe et al., 2004; Dettinger, 2005; Null et al., 2010). For each temperature increase, stream flow was reduced by 14.8 %, 38.3 % and 71.0 % from the base flows measured in July 24, 2012. These flow reductions correspond with the 50th, 25th, and 10th flow percentiles respectively, for the Salmon River (1911–2014, United States Geologic Survey gauge # 11,522,500 Somes Bar, CA, USA). Although stream temperature at the upstream boundary would increase with air temperature in the climate-change scenarios, we had no a priori knowledge of what the model boundary conditions would be under the climate-change scenarios. Thus we performed the climate-change simulations under two different sets of boundary conditions, one that used the hourly stream temperatures observed during the field study and another that applied a uniform air temperature increase of 2 °C to the observed values. This allowed us to assess the sensitivity of the climate-change scenarios to boundary conditions.

2.4.3. Mitigating elevated stream temperature with riparian reforestation

Two reforestation scenarios, named "partial" and "full" reforestation, varied forest canopy heights and densities which were simulated in *Heat Source* to quantify the relative thermal benefit of reforestation compared to climate warming scenarios (Fig. 1). Areas identified for simulated reforesting consisted of denuded gravel bars from historic hydraulic gold mining and areas of low vegetation in the study reach. The partly forested condition increased areas classified as "rock" (no height and no density) to small mixed stand conditions (12 m height, 70 % density) and "willow/shrub/rock" (2 m height, 45 % density) to small conifer stand conditions (12 m height and 45 % density). The fully forested condition increased "rock" and

Fig. 1. Map of vegetation classes for (A) current condition, (B) partial reforestation and (C) full reforestation. Note how grey areas become light and dark green. (For interpretation of the references to color in this figure legend, the reader is referred to the web version of this article.)

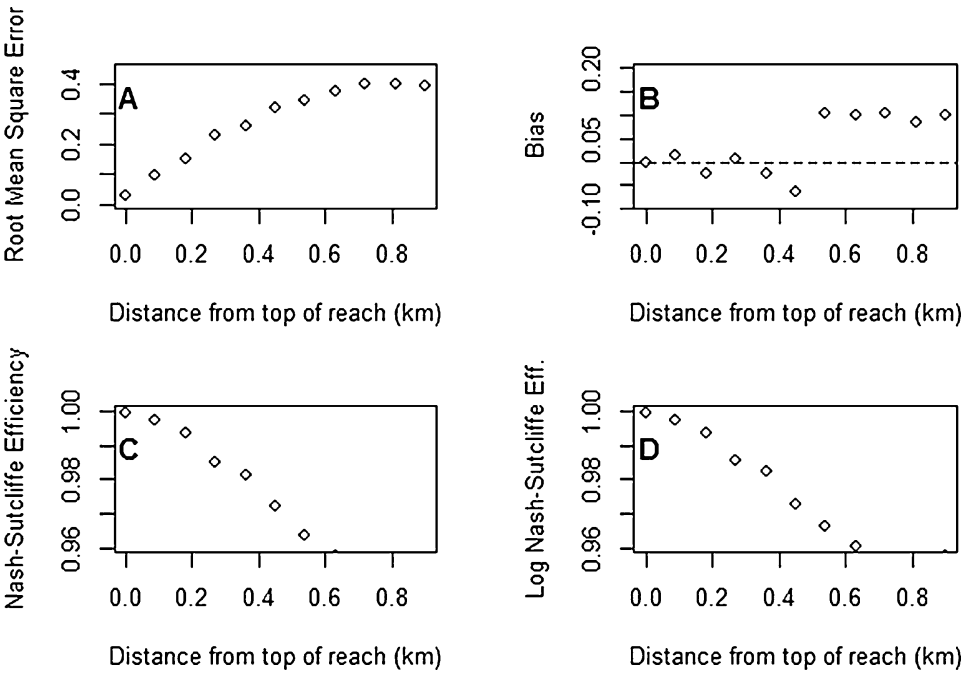

Fig. 2. Model performance metrics at each spatial node, plotted versus distance downstream form the top of the study reach. Each point represents the particular metric, as calculated over the five-day modeling period, July 2012, Salmon River, California, USA.

"willow/shrub/rock" areas to large mixed stand conditions (24 m height and 70 % density) and small conifer stand areas to large conifer stand conditions (27 m height, 70 % density). This condition was used to simulate stand conditions at the end of this century (i.e., 2099), assuming that partially forested stands and extant conifers would continue to grow. To quantify the thermal benefit of reforestation, the mean difference in stream temperature between climate and restored simulations was calculated at the downstream-most spatial node. This allowed us to capture the maximum difference in heating over the study reach.

3. Results

3.1. Model performance

The four measures of model performance indicated very good performance at all nodes, albeit with a general decrease in fit with distance downstream from the top node (Fig. 2). This decrease in fit occurred because temperature boundary conditions were specified at the top node, and the model is driven by observed hourly meteorological conditions, which were recorded only at the top of the reach. Mean bias over all model nodes was 0.036 °C, and bias was a maximum of 0.1 °C in absolute value at each node. Nash-Sutcliffe Efficiency computed on the logarithms was nearly identical to that computed on the raw output (Fig. 2), indicating that large errors did not skew performance measures. Log-NSE was greater than 0.96 at all nodes. The best time series model of error at this node (over 50 % of the AICc weight) consisted of a periodic component with a frequency of 6 cycles per day and first-order autocorrelation of 0.67 between hourly time steps. This statistical characterization of the error clearly showed that *Heat Source* systematically over-predicted water temperature from late morning through mid-afternoon (Fig. 3).

3.2. Mitigating elevated stream temperature with riparian reforestation

Heat Source predicted increases in mean daily average stream temperatures over the study reach of 0.23 °C/km, 0.45 °C/km, and 0.68 °C/km resulting from climate-change-induced increases in mean annual air temperature of 2 °C, 4 °C, and 6 °C, respectively (Table 4). Temperature increases were reduced by 0.11 °C/km under simulated partial reforestation of riparian buffers, and 0.26 °C/km with full reforestation (Table 4). Reforestation thermal profiles highlight the buffering potential of riparian forest during daily maximum temperatures (Fig. 4). Model simulations of flow reductions indicated an overall trend of increasing mean stream temperatures as mean air temperature increased and stream discharge was lowered (Table 4). The greatest warming was observed for the 10th percentile flow under 6 °C of air temperature warming (from baseline conditions of 18.66 °C to 20.02 °C). Interestingly, no differences in mean stream temperatures were observed for flow reductions under the 2 °C scenario. Lower flows resulted in greater heating during peak hours, but this was balanced by higher cooling rates

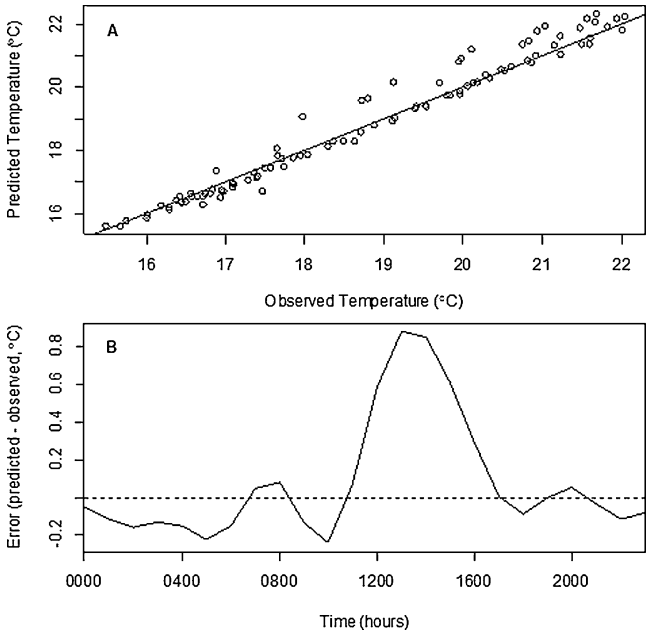

Fig. 3. Model error at the downstream-most node. (A) predicted versus observed temperature values for all hourly observations over the five-day modeling period. Line indicates perfect fit. (B) periodic component of error. Dashed line indicates perfect fit.

during nighttime hours. Accordingly, maximum daily temperatures increased as flow was reduced (Fig. 5), and minimum daily temperatures became lower.

Full reforestation more than doubled the cooling effect on mean daily stream temperatures of partial reforestation. The cooling effect of reforestation increased as the simulated stream discharge was lowered. Cooling effects in the different flow scenarios were similar across increased air temperature scenarios (Table 4). For example, under full reforestation *Heat Source* predicted 0.26–0.27 °C/km cooling under current flows, 0.29–0.31 °C/km with 14.8 % reduction, 0.39–0.40 °C/km cooling with 38.3 % reduction and 0.66-0.68 °C/km cooling with 71.0 % reduction, all regardless of air temperature scenario.

Reforestation lowered maximum daily temperatures in all scenarios, however not always cooling the stream at or below current climactic conditions (Fig. 5). Partial reforestation lowered maximum daily temperatures below baseline for all 2 °C air temperature rise scenarios except the 71.0 % flow reduction scenario. Partial reforestation did not lower daily maximum temperatures in any of the flow reduction scenarios with 4 °C and 6 °C temperature rise. (Fig. 5). Full reforestation lowered maximum temperatures below current conditions under all scenarios except 6 °C temperature rise combined with 71.0 % flow reduction. Daily minimum temperatures were very similar between reforestation scenarios. A slight increase in daily minimum values (~0.06 °C/km) was observed with increased vegetation, possibly due to increased air temperature or increased long-wave radiation from the vegetation. Our sensitivity analysis found no difference in the predictions of warming or buffering from reforestation over the study reach when boundary-condition stream temperatures (inflows to the top of the study reach) were increased by 2 °C over the values observed during the study period.

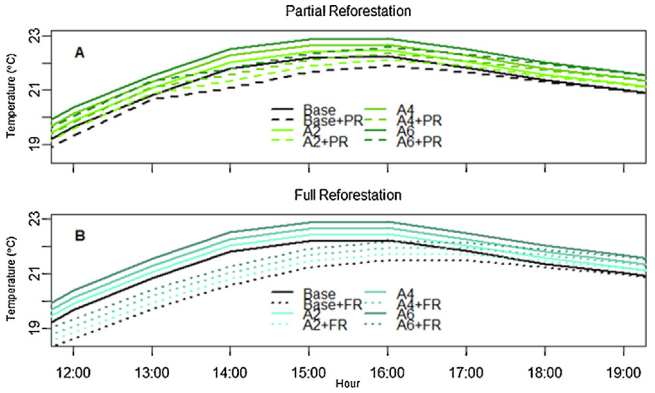

Fig. 4. Thermal profiles comparing warning scenarios without changes in flow (solid lines) with (A) partial reforestation (dashed lines) and (B) full reforestation (dotted lines) during daily maximum betwee 12:00 and 18:00 on July 22nd 2012, Salmon River, California, USA.

Table 4
Modeled climate-change and flow reduction scenarios, resulting stream temperatures, and cooling resulting from with reforestation. Stream warming, reforestation and flow reductions are relative to field conditions measured July 20–24, 2012 on the North Fork Salmon River, CA, USA. Flow reductions of 14.8 %, 38.3 % and 71.0 % correspond to the 50th, 25th and 10th percentile flows for 1911–2014, respectively.

Model scenario	Modeled flow reduction [%]	5 day mean stream temp. [°C/km]	Increase in stream temp. [°C/km]	Partial reforestation [°C/km]	Full reforestation [°C/km]
Baseline	0	18.66	0	−0.110	−0.259
	With 2 °C Increase in mean annual air temperature				
A2	0	18.89	0.225	−0.112	−0.263
A2F15	−14.8	18.89	0.226	−0.122	−0.287
A2F38	−38.3	18.89	0.228	−0.165	−0.387
A2F71	−71.0	18.89	0.226	−0.280	−0.659
	With 4 °C increase in mean annual air temperature				
A4	0	19.12	0.452	−0.115	−0.268
A4F15	−14.8	19.15	0.485	−0.131	−0.305
A4F38	−38.3	19.22	0.561	−0.169	−0.394
A4F71	−−71.0	19.45	0.788	−0.285	−0.669
	With 6 °C increase in mean annual air temperature				
A6	0	19.34	0.681	−0.117	−0.273
A6F15	−14.8	19.41	0.746	−−0.134	−0.311
A6F38	−38.3	19.38	0.897	−0.172	−0.401
A6F71	−71.0	20.02	1.355	−0.291	−0.681

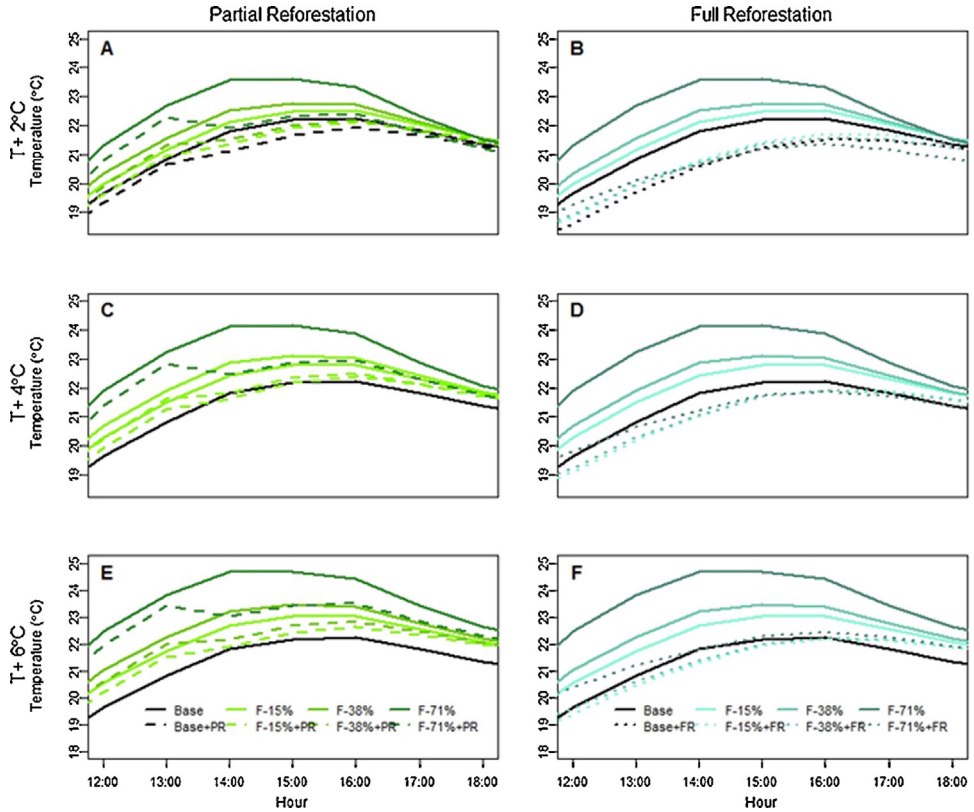

Fig. 5. Thermal profiles comparing warning scenarios (solid lines) with partial reforestation (left panels, dashed lines) and full reforestation (right panels, dotted lines) during daily maximum between 12:00 and 18:00 on July 22nd 2012, Salmon River, California, USA. Flow reductions are represented by each color. The black solid lines are the base (observed 2012) condition. Panels (A) and (B) also include reforestation scenarios with no warning simulated (black dashed and dotted lines respectively).

4. Discussion

4.1. Model performance

Heat Source is a mechanistic model that estimates stream temperature from geomorphic, meteorologic, and hydrologic conditions (Boyd and Kasper, 2003). *Heat Source* was developed to help inform land managers on current and potential

restoration conditions. The four measures of spatial model fit used in this analysis were comparable to previous *Heat Source* applications in Oregon (ODEQ, 2001, 2010; Crown et al., 2008; Crown 2010). Our study focused on matching the entire daily cycle, while *Heat Source* TMDL applications have focused on matching daily maximum temperatures. Had we calibrated our model to match daily maximum temperatures, the systematic over-prediction of afternoon temperatures (Fig. 3) would have been lower, at the cost of overall performance throughout the diel cycle. Our study's Log-NSE is much lower than previous applications, most likely due to small size of the temporal and spatial domains we used. Our study's mean and maximum RMSE are similar to those of other applications of *Heat Source* to small drainages (ODEQ, 2001, 2010). For perspective, our study's maximum RMSE of 0.40 °C is about 8 % of the diel fluctuation (5 °C) observed over the study period.

The spatial pattern showing a decrease in fit in a downstream direction was most likely due to lack of continuous data at the downstream end of the study reach. Both stream flow and meteorological conditions (i.e., wind speed, air temperature, humidity, solar radiation) were measured only at the top of the study reach. While *Heat Source* took the distance from the upstream continuous data node into account, additional meteorological stations at more locations would have increased model fit because the inputs at each spatial location would be more accurate than just using values measured at the upstream node.

One area that required direct calibration of model outputs to match field measurements was the depth and extent of hyporheic exchange. Other studies have highlighted this as an area of uncertainty (Malcolm et al., 2004). *Heat Source* does not explicitly track flows into and out of the subsurface reservoir. DTS has been used to estimate groundwater inflow in previous work and could facilitate future modeling efforts (Westhoff et al., 2011b). Future versions of *Heat Source* would be strengthened by incorporating greater hyporheic flow modeling.

Heat Source further requires an hourly stream temperature boundary condition. Our study did not change this boundary stream temperature condition to reflect climate-change, although we did conduct a sensitivity analysis on boundary conditions. Our investigation focused on the relative change in heating and timing through the study reach rather than the absolute change in temperature. Elevated air temperature is expected to change the initial condition of stream temperature. Our sensitivity analysis found no difference in warming or warming offset between simulations that used observed water temperatures as the boundary conditions and simulations that used boundary conditions that were 2 °C higher than observed values. We concluded that model errors were within an acceptable range and felt confident in using *Heat Source* to investigate climate warming and reforestation scenarios.

4.2. Mitigating elevated stream temperature with riparian reforestation

Riparian zones create microclimates which dynamically interact with energy exchanges between the water–air interface (Moore et al., 2005). Riparian zones provide thermal buffering directly via shading and changes in longwave radiation (Brown and Krygier, 1970; Armour et al., 1991; Fleischner, 1994) as well as indirectly via interacting with channel hydraulics (Andrews, 1984). Our study found that partial and full reforestation of riparian buffers reduced the impacts of climate-change on stream temperatures. Mean daily maximum temperatures were reduced by reforestation while daily minimum temperatures were essentially unchanged. The reduction (0.11–0.12 °C/km and 0.26–0.27 °C/km per 2 °C air temperature increase for partial and fully forested respectfully) is within the same order of magnitude as simulated heating caused by climate-change (0.23 °C/km, 0.45 °C/km, and 0.68 °C/km for mean air temperature increases of 2 °C, 4 °C, and 6 °C respectively). This means that reforesting areas lacking riparian zones (currently denuded gravel bars and areas with little vegetation) not only improves stream temperature related to current conditions but could reduce impacts from future warming conditions under constant boundary conditions. Numerous experiments removing forest vegetation and observing resultant stream warming have been performed, emphasizing the important role of riparian cover in protecting streams from direct insolation (Moore et al., 2005, Webb et al., 2008).

The simulations of reduced stream discharge during peak heating months, representing reduced snowpack, indicated strong increases in mean and maximum daily stream temperatures. The effect increased as the modeled discharge decreased. Interestingly minimum temperatures were lowered under reduced discharge scenarios. Cooling takes place at nighttime when stream water emits more longwave radiation than it is receiving from the landscape and atmosphere. Thus with less water the stream appears to both warm and cool faster. While the buffering effect of reforestation did not change for different air temperatures, it was observed to increase with reduced discharge. For example, a cooling of 0.68 °C/km was observed for 71.0 % flow reduction and 0.31 °C/km for 14.8 % flow reduction under the 6 °C air temperature rise scenario. These results would suggest the additional importance of reforestation as climate warming results in lowered discharges and shifts in snowmelt timing.

Heat Source was parameterized here to model climate-change scenarios of increased average daily temperatures and reduced stream flow. The simulation could be improved by investigating how changes to the diurnal pattern of temperature increase (e.g., greater changes to daily maximum temperatures than to means) affect stream temperature. Other aspects of climate that are expected to change and will influence stream temperature, directly or indirectly will be precipitation, wildfire frequency, discharge, and groundwater inflows, relative humidity, cloudiness, and wind speed and direction. *Heat Source* modeling of forest reforestation is robust as it captures changes to forest canopy and shading more explicitly, with net solar radiation being order of magnitude larger influence on stream temperatures than sensible and latent heat exchange (Moore et al., 2005).

Riparian ecosystems are naturally resilient and may provide an adaptive role in mitigating negative climate-change impacts (Seavy et al., 2009). Our results indicate that land managers can focus initially on matching partially forested conditions for the near future (first half of the 21st century) and see immediate benefits. Fully forested conditions can further buffer stream temperature for the 2099 elevated air temperature scenario. Focusing restoration efforts on reforesting riparian areas have additional ecological benefits such as linking aquatic and terrestrial systems, reducing the impacts of extreme flooding, and possibly creating additional thermal refugia (Seavy et al., 2009). With stream temperatures rising worldwide (e.g., Kaushal et al., 2010) and a continuation of this trend predicted (van Vliet et al., 2013) it is critical to start implementing and testing land management strategies that can potentially ameliorate ecological impacts. There is a need to conduct research that evaluates climate adaptation measures in addition to understanding climate drivers of ecological change (Wilby et al., 2010). Restoration practitioners need to restore ecosystem function as well as adapt to climate-change and enhance ecological resilience (Millar et al., 2007; Heller and Zavaleta, 2009).

5. Conclusions

The model *Heat Source* was successful in simulating stream heating during critical low flow time periods, July 20–24, 2012 for salmonid species in the North Fork of the Salmon River, CA USA as measured by four measures of model fitness to temperature data collected using distributed temperature sensing technology. The effect of elevated air temperature on mean and maximum daily stream temperatures resulting from climate-change was predicted. Results indicate a 0.23 °C/km, 0.45 °C/km and .68 °C/km increase in mean stream temperature resulting from 2 °C, 4 °C and 6 °C of air temperature rise relative to current conditions. Simulations of partial reforestation of riparian forest degraded by historic gold mining offset this warming by cooling 0.11–0.12 °C/km for the partial and 0.26–0.27 °C/km for the full reforestation scenario for all three air temperature increases. Minimum temperatures were slightly raised by reforestation. Model results indicate that lower summertime streamflow from reduced snowpack and earlier snowmelt will result in higher peak stream temperatures. This warming could be mitigated by reforestation. However under the most severe flow reduction and warming scenarios (6 °C air temperature increase, 71.0 % flow reduction), only half the predicted stream warming for this site would be reduced by the full reforestation scenario. Mitigating stream temperatures is important because peak temperatures are already exceeding tolerance limits for salmonid species. Land managers investigating “thermal hotspots” should consider reforestation as a tool for mitigating both current and future warming.

Acknowledgements

Funding was provided by the USDA McIntire-Stennis Program, Project # CALZ-154. We gratefully acknowledge the help of Oregon Department of Environmental Quality, Salmon River Restoration Council, Widgets of Science, and the Center for Transformative Environmental Monitoring Programs. We are also grateful for the help of Dr. Darren Ward (Humboldt State University), our dedicated field crew, and Salmon River residents. We are indebted to two anonymous reviewers for their comments which strengthened earlier drafts of this manuscript.

Appendix A. Supplementary data

Supplementary data associated with this article can be found, in the online version, at http://dx.doi.org/10.1016/j.ejrh.2015.07.002.

References

AFL Telecommunications. 2007. Fiber Optic Cable Specification Sheet. http://www.aflglobal.com/Products/Fiber-Optic-Cable/ADSS/Drop-Cable/Flat_Drop_Cable.aspx (accessed: 01.22.13.).

Ando, C.J., Irwin, W.P., Jones, D.L., Saleeby, J.B., 1983. The ophiolitic North Fork terrane in the Salmon River region, central Klamath Mountains, California. Geol. Soc. Am. Bull. 94, 236.

Andrews, E.D., 1984. Bed-material entrainment and hydraulic geometry of gravel-bed rivers in Colorado. Geol. Soc. Am. Bull. 95, 371–378, http://dx.doi.org/10.1130/0016-7606(1984)95<371:BEAHGO>2.0.CO;2.

Arcement, G.J., Schneider, V.R., 1989. Guide for selecting Manning's roughness coefficients for natural channels and floodplains. US Geol. Surv., Water-Supply Paper, 2339.

Armour, C.L., Duff, D.A., Elmore, W., 1991. The effects of livestock grazing on riparian and stream ecosystems. Fisheries 16, 7–11.

Battin, J., Wiley, M.W., Ruckelshaus, M.H., Palmer, R.N., Korb, E., Bartz, K.K., Imaki, H., 2007. Projected impacts of climate-change on salmon habitat restoration. Proc. Natl. Acad. Sci. 104, 6720–6725, http://dx.doi.org/10.1073/pnas.0701685104.

Berman, C.H., Quinn, T.P., 1991. Behavioural thermoregulation and homing by spring chinook salmon, *Oncorhynchus tshawytscha* (Walbaum), in the Yakima River. J. Fish Biol. 39, 301–312.

Bond, RM. Using Distributed Temperature Sensing Fiber-optics and Heat Source Modeling to Characterize a Northern California Stream's Thermal Regime. 2013. M. S. Thesis. Dept Forestry and Wildland Res. Humboldt State Univ. CA, USA, <http://hdl.handle.net/2148/1645>.

Boyd M., Kasper B. 2003. Analytical methods for dynamic open channel heat and mass transfer: methodology for the Heat Source Model Version 7.0, Watershed Sciences Inc., Portland, Oregon. found at: <http://www.heatsource.info/Heat> Source v 7.0.

Brown, G.W., Krygier, J.T., 1970. Effects of clear-cutting on stream temperature. Water Resour. Res. 6, 1133–1139.

Burnham, K.P., Anderson, D.R., 2004. Multimode inference: understanding AIC and BIC in model selection. Sociol. Method Res. 33, 261–304, http://dx.doi.org/10.1177/0049124104268644.

California Environmental Protection Agency (CA EPA). 2002. Section 303(d) List Fact Sheet for California.

Caissie, D., 2006. The thermal regime of rivers: a review. Freshwater Biol. 51, 1389–1406, http://dx.doi.org/10.1111/j.1365-2427.2006.01597.x.

Crown, J., Meyers, B., Turgaw, H., Turner, D., 2008. Rogue River Basin Total Maximum Daily Load (TMDL): Appendix A, Temperature Calibration. Technical Report. Oregon Department of Environmental Quality, Portland, Oregon.
Crown, J., 2010. John Day River Basin Total Maximum Daily Load (TMDL) and Water Quality Management Plan (WQMP) Technical Report: Appendix A: Temperature Model Calibration Report. Technical Report. Oregon Department of Environmental Quality, Portland, Oregon.
Dettinger, M.D., 2005. From climate-change spaghetti to climate-change distributions for 21st Century California. San Francisco Estuary Watershed Sci. 3.
Diabat, M., Haggerty, R., Wondzell, S.M., 2012. Diurnal timing of warmer air under climate-change affects magnitude, timing and duration of stream temperature change. Hydrol. Process. 27, 2367–2378, http://dx.doi.org/10.1002/hyp.9533.
Eaton, J.G., Scheller, R.M., 1996. Effects of climate warming on fish thermal habitat in streams of the United States. Freshwater Ecosys. Climate-change in N. Am. 41, 1109–1115.
Elder, D., Olson, B., Olson, A., Villeponteaux, J., Brucker, P. 2002. Salmon River Subbasin Restoration Strategy: Steps to Recovery and Conservation of Aquatic Resources. U.S. Fish & Wildlife Service, The Klamath River Basin Fisheries Restoration Task Force (Interagency Agreement 14-48-11333-98-H019).
Environmental Protection Agency (EPA). 2006. EMAP Western Pilot Study Operations Manual for Wadeable Streams, Peck, DV, Lazorchak JM, and DJ Klemm, editors. Washington, D.C.
Environmental Systems Research Institute (ESRI). 2011. World Imagery Basemap website: <http://www.arcgis.com/home/item.html?id=10df2279f9684e4a9f6a7f08febac2a9>.
Federal Register. 1997. Endangered and Threatened Species: Threatened status for coho salmon in the Southern Oregon/ Northern California Evolutionary Significant Unit in California. Federal Register, Washington D.C. 62: 24588–24609.
Fleischner, T.L., 1994. Ecological costs of livestock grazing in western North America. Conserv. Biol. 8, 629–644.
Freeze, R.A., Cherry, J.A., 1979. Groundwater. Prentice-Hall, Englewood Cliffs, NJ.
Gregory, J.S., Beesley, S.S., Van Kirk, R.W., 2000. Effect of springtime water temperature on the time of emergence and size of Pteronarcys californica in the Henry's Fork catchment, Idaho, U. S. A. Freshwater Biol. 45, 75–83, http://dx.doi.org/10.1046/j.1365-2427.2000.00619.x.
Hill, R.A., Hawkins, C.P., Jin, J., 2014. Predicting thermal vulnerability of stream and river ecoysytems to climate-change. Climatic Change 125, 399–412, http://dx.doi.org/10.1007/s10584-014-1174-4.
Hannah, D.M., Malcolm, I.A., Soulsby, C., Youngson, A.F., 2008. A comparison of forest and moorland stream microclimate, heat exchanges and thermal dynamics. Hydrol. Process. 22, 919–940, http://dx.doi.org/10.1002/hyp.7003.
Hausner, M.B., Suárez, F., Glander, K.E., van de Giesen, N., Selker, J.S., Tyler, S.W., 2011. Calibrating single-ended fiber-optic raman spectra distributed temperature sensing data. Sensors 11, 10859–10879, http://dx.doi.org/10.3390/s111110859.
Hayhoe, K., Cayan, D., Field, C., Frumhoff, P., Maurer, E., Miller, N., Moser, S., Schnider, S., Nicholas Cahill, K., Cleland, E., Dale, L., Drapek, R., Hanemann, M., Kalkstein, L., Lenihan, J., Lunch, C., Nielson, R., Sheridan, S., Verville, J., 2004. Emissions pathways, climate-change, and impacts on California. Proc. Natl. Acad. Sci. 101, 12422–12427, http://dx.doi.org/10.1073/pnas.0404500101.
Heller, N.E., Zavaleta, E.S., 2009. Biodiversity management in the face of climate-change: a review of 22 years of recommendations. Biol. Conserv. 142, 14–32, http://dx.doi.org/10.1016/j.biocon.2008.10.006.
International Panel on Climate-change (IPCC). 2007. Climate-change 2007: The Physical Science Basis. Contribution of Working Group I to the Fourth Assessment Report of the Intergovernmental Panel on Climate-change [S., Solomon, D., Qin, M., Manning, Z., Chen, M., Marquis, K.B., Averyt, M. Tignor, H.L. Miller (eds.)]. Cambridge University Press, Cambridge, United Kingdom and New York, NY, USA.
Kaushal, S.S., Likens, G.E., Jaworski, N.A., Pace, M.L., Sides, A.M., Seekell, D.R., 2010. Rising stream and river temperatures in the United States. Fronts Ecol. Environ., http://dx.doi.org/10.1890/090037.
Lowney, C.L., 2000. Stream temperature variation in regulated rivers: Evidence for a spatial pattern in daily minimum and maximum magnitudes. Water Resour. Res. 36, 2947–2955, http://dx.doi.org/10.1029/2000WR900142.
Malcolm, I.A., Hannah, D.M., Donaghy, M.J., Soulsby, C., Youngston, A.F., 2004. The influence of riparian woodland on the spatial and temporal variability of stream water temperatures in an upland salmon stream. Hydrol. Earth Sys. Sci. 8, 449–459, http://dx.doi.org/10.5194/hess-8-449-2004.
Markarian, R.K., 1980. A study of the relationship between aquatic insect growth and water temperature in a small stream. Hydrobiologia 75, 81–95.
Matheswaran, K., Blemmer, M., Mortensen, J., Rosbjerg, D., Boegh, E. 2011. Investigating the effect of surface water-groundwater interactions on stream temperature using Distributed temperature sensing and instream temperature model. In Conceptual and Modelling Studies of Integrated Groundwater, Surface Water, and Ecological Systems, Proceedings of Symposium H01 held during IUGG2011 in Melbourne, Australia.
Matthews, K.R., Berg, N.H., 1997. Rainbow trout responses to water temperature and dissolved oxygen stress in two southern California stream pools. J. Fish Biol. 50, 50–67.
Meisner, J.D., 1990. Effect of climatic warming on the southern margins of the native range of brook trout, Salvelinus fontinalis. Can. J. Fish. Aquatic Sci. 47, 1065–1070.
Millar, C.I., Stephenson, N.L., Stephens, S.L., 2007. Climate-change and forests of the future: managing in the face of uncertainty. Ecol. Appl. 17, 2145–2151, http://dx.doi.org/10.1890/06-1715.1.
Mohseni, O., Heinz, S., Eaton, J., 2003. Global warming and potential changes in fish habitat in U. S. streams. Climatic Change 59, 389–409, http://dx.doi.org/10.1023/A.1024847723344.
Moore, R.D., Spittlehouse, D.L., Story, A., 2005. Riparian microclimate and stream temperature response to forest harvesting: a review. J. Am. Water Res. Association 41, 813–834, http://dx.doi.org/10.1111/j.1752-1688.2005.tb03772.x.
National Marine Fisheries Service. 2012. Public Draft Recovery Plan for Southern. Oregon/Northern California Coast Coho Salmon (*Oncorhynchus kisutch*). National Marine Fisheries Service Arcata, California.
National Research Council. 2004. Endangered and threatened fishes in the Klamath River Basin: causes of decline and strategies for recovery. Technical Report.
Null, S.E., Viers, J.H., Mount, J.F., 2010. Hydrologic Response and Watershed Sensitivity to Climate Warming in California's Sierra Nevada. PLoS ONE 5 (4), e9932, http://dx.doi.org/10.1371/journal.pone.0009932.
Null, S.E., Viers, J.H., Deas, M.L., Tanaka, S.K., Mount, J.F., 2013. Stream temperature sensitivity to climate warming in California's Sierra Nevada: impacts to coldwater habitat. Climatic Change 116, 149–170, http://dx.doi.org/10.1007/s10584-012-0459-8.
Oregon Department of Environmental Quality (ODEQ). 2001. UmatillaRiver Basin Total Maximum Daily Load (TMDL) and Water Quality Management Plan (WQMP): Appendix A-4: Temperature Technical Analysis. Technical Report, Oregon Department of Environmental Quality.
ODEQ. 2010. Upper Grande Ronde Sub-Basin TMDL. Appendix A Temperature Analysis: Thermal Patterns, Source Assessment and Analytical Framework. Technical Report, Oregon Department of Environmental Quality.
ODEQ. 2012. Heat Source version 7.0, <http://www.deq.state.or.us/wq/tmdls/tools.htm>.
Poole, G.C., Berman, C.H., 2001. An ecological perspective on in-stream temperature: natural heat dynamics and mechanisms of human-caused thermal degradation. Environ. Manage. 27, 787–802, http://dx.doi.org/10.1007/s002670010188.
Roth, T.R., Westhoff, M.C., Huwald, H., Huff, J.A., Rubin, J.F., Barrenetxea, G., Vetterli, M., Parriaux, A., Selker, J.S., Parlange, M.B., 2010. Stream temperature response to three riparian vegetation scenarios by use of a distributed temperature validated model. Environ. Sci. Technol. 44, 2072–2078, http://dx.doi.org/10.1021/es902654f.
Solomon, S., Qin, D., Manning, M., Chen, Z., Marquis, M., Averyt, K.B., Tignor, M., Miller, H.L., 2007. Contribution of Working Group I to the Fourth Assessment Report of the Intergovernmental Panel on Climate-change. Chapter 10.5.4. Cambridge University Press, United Kingdom.
Seavy, N.E., Gardali, T., Golet, G.H., Griggs, T.F., Howell, C.A., Kelsey, R., Small, S.L., Viers, J.H., Weigand, J.F., 2009. Why climate-change makes riparian restoration more important than ever: recommendations for practice and research. Ecol. Restor. 27, 330–338, http://dx.doi.org/10.3368/er.27.3.330.

Selker, J.S., Thévenaz, L., Huwald, H., Mallet, A., Luxemburg, W., van de Giesen, N., Stejskal, M., Zeman, J., Westhoff, M., Parlange, M.B., 2006a. Distributed fiber-optic temperature sensing for hydrologic systems. Water Resour. Res., WR005326, http://dx.doi.org/10.1029/2006WR005326.
Selker, J., van de Giesen, N., Westhoff, M., Luxemburg, W., 2006b. MB Parlange. Fiber optics opens window on stream dynamics. Geophys. Res. Lett., GL027979, http://dx.doi.org/10.1029/2006GL027979.
Shumway, R.H., Stoffer, D.S., 2011. Time Series Analysis and its Applications, 3rd edition. Springer, New York.
Tyler, S.W., Selker, J.S., Hausner, M.B., Hatch, C.E., Torgersen, T., Thodal, C.E., Schladow, S.G., 2009. Environmental temperature sensing using Raman spectra DTS fiber-optic methods. Water Resour. Res., WR007052, http://dx.doi.org/10.1029/2008WR007052.
U.S. Department of Agriculture (USDA), Forest Service. 2006. Region 6 Stream Inventory Handbook, Level II, Version 2.6.
van Vliet, M.T.H., Franssen, W.H.P., Yearsley, J.R., Ludwig, F., Haddeland, I., Lettenmaier, D.P., Kabat, P., 2013. Global river discharge and water temperature under climate-change. Global Environ. Change 23, 450–464.
Webb, B.W., Hannah, D.M., Moore, R.D., Brown, L.E., Nobilis, F., 2008. Recent advances in stream and river temperature research. Hydrol. Process 22, 902–918, http://dx.doi.org/10.1002/hyp.6994.
Welsh, H., Hodgson, G., Harvey, B., Roche, M., 2001. Distribution of Juvenile Coho Salmon in Relation to Water Temperatures in Tributaries of the Mattole River, California. North American Journal of Fisheries Management 21, 464–470, http://dx.doi.org/10.1577/1548-8675(2001)021<0464:DOJCSI>2.0.CO;2.
Westhoff, M.C., Savenije, H.H.G., Luxemburg, W.M.J., Stelling, G.S., Van De Giesen, N.C., Selker, J.S., Pfister, L., Uhlenbrook, S., 2007. A distributed stream temperature model using high resolution temperature observations. Hydrol. Earth Sys. Sciences 11, 1469–1480, http://dx.doi.org/10.5194/hessd-4-125-2007.
Westhoff, M.C., Savenije, H.H.G., Luxemburg, W.M.J., Stelling, G.S., Van De Giesen, N.C., Selker, J.S., Pfister, L., Uhlenbrook, S., 2011a. Corrigendum to A distributed stream temperature model using high resolution temperature observations published in Hydrol. Earth Syst. Sci. 11, 1469–1480.
Westhoff, M.C., Gooseff, M.N., Bogaard, T.A., Savenije, H.H.G., 2011b. Quantifying hyporheic exchange at high spatial resolution using natural temperature variations along a first-order stream. Water Resour. Res., WR009767, http://dx.doi.org/10.1029/2010WR009767.
Wilby, R.L., Orr, H., Watts, G., Battarbee, R.W., Berry, P.M., Chadd, R., Dugdale, S.J., Dunbar, M.J., Elliott, J.A., Extence, C., Hannah, D.M., Holmes, N., Johnson, A.C., Knights, B., Milner, N.J., Ormerod, S.J., Solomon, D., Timlett, R., Whitehead, P.J., Wood, P.J., 2010. Evidence needed to manage freshwater ecosystems in a changing climate: turning adaptation principles into practice. Sci. Total Environ. 408, 4150–4164, http://dx.doi.org/10.1016/j.scitotenv.2010.05.014.